Proceedings of The Institute of Acoustics

MODELLING OF A PRESSURE GRADIENT CARDIOID HYDROPHONE

B. Stupfel, C. Granger and J.N. Decarpigny

Acoustics Laboratory⁺, Institut Supérieur d'Electronique du Nord
41, Boulevard Vauban, 59046 Lille Cedex, France

INTRODUCTION

A pressure-gradient cardioïd hydrophone has been designed in our laboratory [1], [2] with a special emphasis to obtain a large bandwidth, though its geometrical dimensions are well below the wavelength. It can be schematically described as a stainless steel cylinder including at its front face a trilaminar piezoelectric disk and at its back face a phaseshift acoustic circuit (oil filled cavity and thin annular slot). Several theoretical attempts are made in order to model this hydrophone, taking account of the diffraction effects. In a first step, an integral formulation is used to solve the Helmholtz equation, while the steel housing is considered as perfectly rigid and the trilaminar disk and phase shifter are represented by lumped constant acoustic circuits [2,3,4]. Comparison with experimental results is disappointing, though nice results are obtained with a simpler device. So, to overcome the hypothesis of a perfectly rigid housing, a three-dimensional modelling of the solid part of the hydrophone is performed [4], using the finite element code ATILA [5,6]. Comparison with experimental results, obtained in the case of an in-air modal analysis, is satisfactory. Work is now in progress to model the complete hydrophone and to solve the whole diffraction problem by coupling the finite element code and the integral equation formulation.

HYDROPHONE DESIGN

The hydrophone (Fig. 1) is a stainless steel cylinder (40 mm OD, 14 mm high) including on its front face a trilaminar piezoelectric disk isolated from the surrounding fluid by a thin polyurethane film. The trilaminar disk is

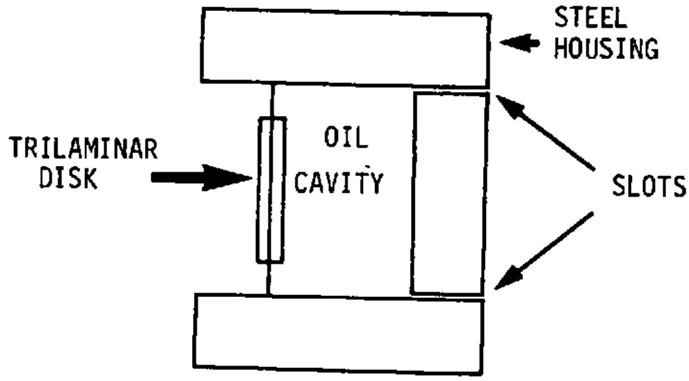

Fig. 1 - Schematic description of the cardioïd hydrophone

constituted of an aluminium alloy core on each side of which two titanozirconate piezoelectric ceramic disks having parallel polarization are cemented. The disks are connected in parallel so that the output voltage signal is maximum when the trilaminar disk has a flexural motion. An oil filled cavity and three narrow annular slots 0.3 mm thin , which are sealed off from the surrounding medium by a thin rubber membrane, are provided in the rear housing ; the cavity and the slots consitute the phase shift acoustic system. The three 120° apart mechanical bridges ensure the binding between the back and lateral faces of the steel housing. For convenience, they are not represented on Fig. 1.

LUMPED CONSTANT ACOUSTIC CIRCUIT AND INTEGRAL EQUATION FORMULATION MODELLING

Given an incident plane wave $p^i(\underline{r}) = p^i e^{i(\underline{k}\cdot\underline{r}-\omega t)}$ impinging on the hydrophone along a direction making an angle θ with the Oz axis of the cylinder, our aim is to compute the output voltage V_S (θ,f) in a given frequency range and to compare it to the experimental results. In this section, we only consider the cases θ = 0° or θ = 180°, knowing that when θ = 0°, the plane wave impinges on the trilaminar disk. We assume in this section that Oz is a revolution axis for the hydrophone, so that the whole problem is two- dimensional. Furthermore, we make the following assumptions : i) the steel housing is a perfectly rigid cylinder including on its front face the trilaminar disk considered as a plane circular piston ; ii) the oil-filled cavity is considered as a frequency independent acoustic capacity and iii) the oil flow is laminar throughout the slot.

Before we deal with the complete hydrophone, we present results obtained for the following, more simple, device : the rear cavity is filled with air and the slots are suppressed, so that the corresponding hydrophone has no phase shift acoustic system and the steel housing is more rigid. Besides, a polystyrene circular plate is stuck to the back face of the hydrophone, in order to reinforce the acoustic decoupling of the cavity. Considering the hypotheses mentioned above, the motions of the trilaminar disk and cylindrical housing - we take into account a possible rigid motion of this one due to the radiation pressure - are given by the following equations :

$$- i\omega M v_c = F_c + v_T \left(R + i\frac{k_T}{\omega}\right) \qquad (1)$$

$$- i\omega M_T (v_c + v_T) = F_T - v_T \left(R + i\frac{k_T}{\omega}\right) \qquad (2)$$

M(M_T) is the steel cylinder (trilaminar disk) equivalent mass ; v_c(v_c+ v_T) is the displacement velocity of the cylinder (trilaminar disk) ; F_c(F_T) is the pressure force applied to the cylinder (trilaminar disk) :

$$F_C = - \int_{S_+} p(\underline{r})d\underline{r} + \int_{S_-} p(\underline{r})d\underline{r} - F_T$$

MODELLING OF A PRESSURE GRADIENT CARDIOID HYDROPHONE

$$F_T = -\int_{S_T} p(\underline{r})d\underline{r}$$

where S_+, S_- and S_T are respectively the cylinder front face, cylinder back face and trilaminar disk surfaces ; $p(\underline{r})$ is the total pressure at point $\underline{r}$. The lumped circuit constants R and k_T describe the mechanical and piezoelectric behaviour of the trilaminar disk as well as the binding between this one and the steel housing. When $v_c = 0$ (i.e. M is infinite), equations (1) and (2) correspond with the right part of the electroacoustical circuit represented on Fig. 2

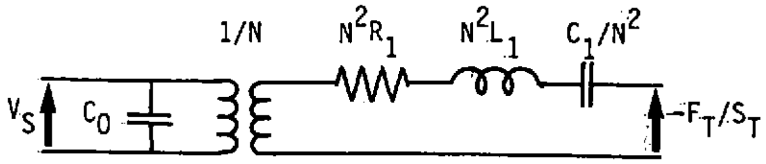

Fig. 2 - Electroacoustical circuit of the fixed, simplified hydrophone.

$(-\ F_T/\ S_T)$ is the average pressure applied to the trilaminar disk ; N is the electroacoustical transformation ratio and R_1, L_1, C_1, C_0 are electrical quantities with :

$$R = R_1(S_TN)^2 \tag{3a}$$

$$k_T = \left(\frac{1}{C_1} + \frac{1}{C_0}\right)(NS_T)^2 \tag{3b}$$

$$M_T = L_1\ (NS_T)^2 \tag{3c}$$

This lumped constant circuit ensures (i) identical displacement velocities on each side of the trilaminar disk and (ii) that V_S is proportional to v_T :

$$V_S = \frac{NS_T\ v_T}{i\omega\ C_0} \tag{4}$$

The values of C_0, C_1, L_1, R_1 are obtained from in-air measurements ($F_T = 0$) of the electrical impedance of the device at the resonance and antiresonance frequencies [2]. The good agreement between the impedance values computed from this circuit and those obtained from in-air measurements ensures the validity of this lumped constant circuit at least in the studied frequency range [2].

At this stage, the unknown quantities are N and the surface pressure $p(\underline{r})$. In the upper part of the studied frequency range, the geometrical dimensions of the device are not small compared with the wavelength of the incident wave, so that a computation of $p(\underline{r})$ taking account of the diffraction effects must be performed. For this purpose, we use the well known integral equation

$$\alpha(\underline{r})\ p(\underline{r}) = p^{i}(\underline{r}) + \int_{S} p(\underline{r}')\ \partial n'\ g(\underline{r},\underline{r}')d\underline{r}' - i\omega\rho\int_{S} v_{n}(\underline{r}')\ g(\underline{r},\underline{r}')\ d\underline{r}'$$

where $\underline{r}$ is a point on S, $g(\underline{r},\underline{r}') = e^{ik|\underline{r}-\underline{r}'|}/4\pi|r-r'|$ and $\partial n'$ stands for $\underline{\nabla}'.\underline{n}'$, n' being the outward normal to S at point $\underline{r}'$; $\alpha(\underline{r}) = 1/2$ when $\underline{r}$ is a regular point of S, v_n ($\underline{r}'$) is the normal surface velocity and ρ the fluid density modulus. Assuming the trilaminar disk and the cylinder to be perfectly rigid, we then have :

$$\alpha(\underline{r})\ p(\underline{r}) = p^{i}(\underline{r}) + \int_{S} p(\underline{r}')\ \partial n' g\ (\underline{r},\underline{r}')\ d\underline{r}' - i\omega\rho\ v_{T}\int_{S_T} g(\underline{r},\underline{r}')\ d\underline{r}' - \ldots$$

$$\ldots - i\omega\rho\ v_{C}\left[\int_{S_+} g(\underline{r},\underline{r}')d\underline{r}' - \int_{S_-} g(\underline{r},\underline{r}')\ d\underline{r}'\right] \qquad \underline{r} \in S \qquad (5)$$

An approximate solution of (5) (see e.g. ref. [7]) is obtained by dividing S into N subdivisions S_i, over each of which the surface pressure is taken equal to a constant p_i. Then $\underline{r}$ in (5) is allowed to take N different values r_i, each of which is the middle of Si, so that $\alpha(\underline{r}_i) = 1/2$. Thus (5) is converted into a (N x N) system of linear equations

$$\frac{1}{2}\, p_i = p_i^{i} + \sum_{j=1}^{N} p_j \int_{S_j} \partial n' g\ (\underline{r}_i,\underline{r}')d\underline{r}' - i\omega\rho\ v_T \int_{S_T} g(\underline{r}_i,\underline{r}')\ d\underline{r}' - \ldots..$$

$$\ldots - i\omega\rho\ v_C\left[\int_{S_+} g(\underline{r}_i,\underline{r}')d\underline{r}' - \int_{S_-} g(\underline{r}_i,\underline{r}')dr'\right] \qquad 1 \leqslant i \leqslant N \qquad (6)$$

The integrals are computed using a Gauss-Legendre quadrature rule, special care being taken when $\underline{r}_i$ belongs to the integration surface. Solving the set of simultaneous equations (1),(2),(6) and (4), we obtain the values of v_T,v_C, $p(\underline{r})$ and V_S for a given frequency, provided this frequency is lower than the first eigenvalue of the associated Dirichlet problem, which is always verified here. The electroacoustical transformation ratio N is considered as a parameter - the only one in this model - and is determined so that the computed resonance frequency f_0 of the hydrophone is equal to the measured resonance frequency. We have reported on Fig. 3 the experimental and computed values of $|V_S(f)/p^i|$ vs frequency with N = 660 Pa/V and $\theta = 0°$; in-air measurements of N performed for this hydrophone yields about 700 Pa/V [2]. We observe a good agreement between computed and experimental values except in the low frequency range, which is rather surprising since diffraction effects are negligible for $f \lesssim 0.46\ f_0$. This discrepancy between computed and measured values is due to the fact that we have neglected the influence of the polystyrene plate [8]. If we assume that this plate behaves like a plane circular piston of radius a (a is the cylinder radius) and of negligible mass, then its in-air resonance frequency is very high. However, when the hydrophone

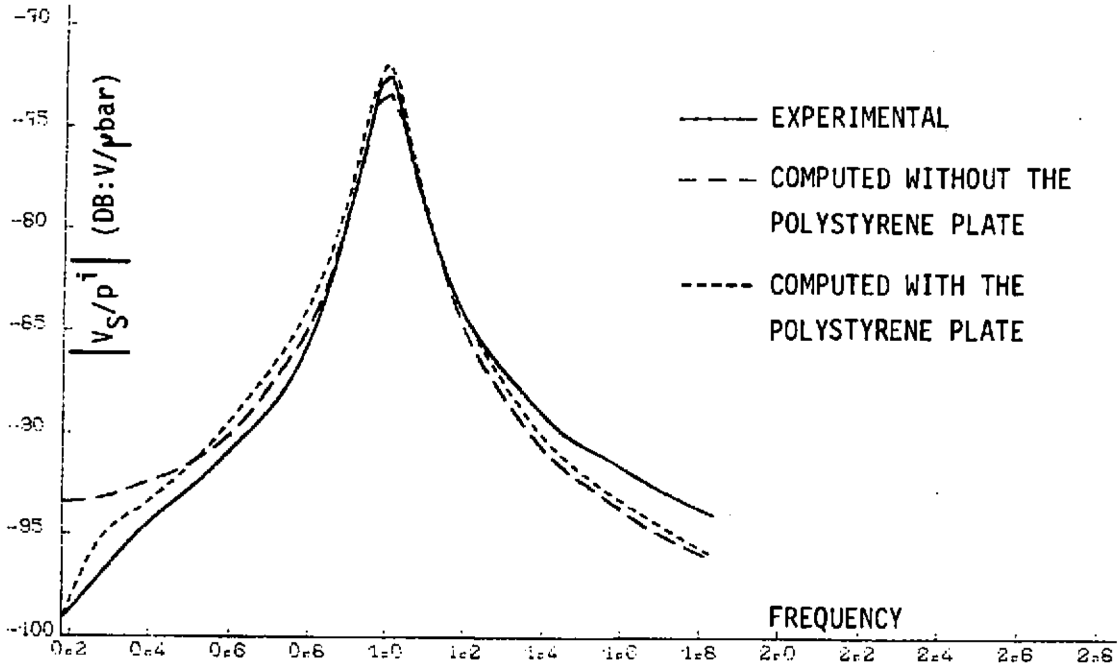

Fig. 3 - $V_S(f, \theta = 0°)$ for the simplified hydrophone

is immersed in fluid, the added fluid mass M_a must be taken into account : if we take $M_a \simeq 8\rho\, a^3/3$ [9], then the resonance frequency f_p of the plate is approximately $(k/M_a)^{½}/2\pi$ where k represents the elasticity of the plate, so that $f_p \simeq 0.1\, f_0$. Indeed, low frequency measurements of V_S performed for this hydrophone [8] show a well defined resonance frequency situated at 0.13 f_0, immediately followed by a pronounced drop of $V_S(f)$ up to about 0.55 f_0. Moreover, if we include the polystyrene plate into the previous model - Eq.(1), (2), (6) and (4) -, the plate being characterized by the mechanical quantity k and the surface S_-, then the low frequency behaviour of V_S is well reproduced (see Fig. 3) [4] : the presence of the polystyrene plate on the rear face of the hydrophone is clearly at the origin of the phenomenon.

If we attempt to model the complete cardioïd hydrophone [2,3], then the equations of motion for the trilaminar disk and cylindrical housing are :

$$- i\omega\, M_C v_C = F_C + v_T \left(R + i\,\frac{k_T}{\omega}\right) - p_C S_T + S_S(p_C - p_S)$$

$$- i\omega\, M_T(v_C + v_T) = F_T - v_T \left(R + \frac{ik_T}{\omega}\right) + p_C\, S_T$$

p_C is the (constant) pressure in the oil cavity, S_S the slot surface and p_S the surrounding fluid pressure on the outward slot surface. p_C is given by :

$$p_C = - \frac{1}{i\omega C'} [S_S \ (v-v_C) - S_T \ v_T]$$

where C' is the acoustical capacity of the oil cavity and v the average fluid velocity in the slot. Finally, the pressure drop between the slot extremities is [3] :

$$p_S - p_C = S_S Z_S \ (v - v_C) - i\omega\rho_S \ \ell_s v_C$$

where ℓ_s is the slot length, ρ_S the oil density modulus and $Z_S = R_s - i\omega L_S$ is the slot impedance taking into account the oil viscosity. Moreover, we must add to (6) the term $i\omega\rho(v - v_C) \int_{S_S} g(\underline{r}_i, \underline{r}') \, dr'$ accounting for the oil flow in the slot. Solving the corresponding set of simultaneous equation, we compute $V_S(f)$ through (4) ; hereagain, N is the only parameter. This lumped constant circuit model induces two resonance frequencies f_1 and f_2 corresponding to the trilaminar disk + cylindrical housing and phase shift system coupled oscillators, the lowest of these frequencies, f_1, being strongly damped on account of the large value of R'. If we take N = 700 Pa/V, which is the experimentally estimated value, then we find a discrepancy of 20 per cent between the computed and measured values of f_2. Besides, these values agree only for $N \gtrsim 1200$ Pa/V, which is not physically admissible. This means that at least one of the hypotheses on which this model is built is not verified. Through a finite element modelling, we have first investigated the perfectly rigid body hypothesis.

FINITE ELEMENT MODELLING

In this section, we present the finite element in-air modelling of the solid part of the three dimensional cardioïd hydrophone, using the finite element code ATILA. We neglect piezoelectric effects, so that the eigenmodes of this device are solutions of the following linear system [5] :

$$([K] - \omega^2 \ [M]) \ \underline{u} = \underline{0}$$

[K] and [M] are respectively the stiffness and mass matrices of the solid structure. The vector $\underline{u}$ represents the nodal values of the displacement field.

The hydrophone admits a symmetry plane normal to the Z axis, so that the displacement field is either symmetrical or antisymmetrical with respect to this plane. Thereby, only one half of the structure has been modelled, and boundary conditions have been prescribed to select symmetrical or antisymmetrical modes. The steel cylindrical housing is modelled by 20 nodes parallelepipedic and 15 nodes prismatic solid elements while 6 and 8 nodes shell elements are used to represent the trilaminar disk (see Fig. 4). The number of degrees of freedom in the symmetrical (antisymmetrical) case is 1211 (1103). The first measured and computed eigenfrequencies of the structure, normalized to the measured frequency of the fundamental mode, are reported in the table below (S and A stand respectively for symmetrical and antisymmetrical) :

Mode	1S	2S	1A	3S	4S	2A	3A	5S	4A	6S
Computed normalized frequency	1.03	1.69	1.70	1.76	1.86	1.87	2.14	2.14	2.40	2.41
Measured normalized frequency	1	1.48	-	1.92	-	-	-	-	-	-

The corresponding mode shapes are represented on Fig. 5 - for clarity's sake, the trilaminar disk is represented separately. Modes 1S and 5S-3A are respectively the first and second eigenmodes of the trilaminar disk ; the others are eigenmodes of the steel housing. Modes 2S, 4S, 5S and 6S are all nearly antisymmetrical with respect to a plane containing the Z axis, so that their computed eigenfrequencies are very close to those of the corresponding antisymmetrical modes 1A, 2A, 3A and 4A. The eigenfrequencies have been

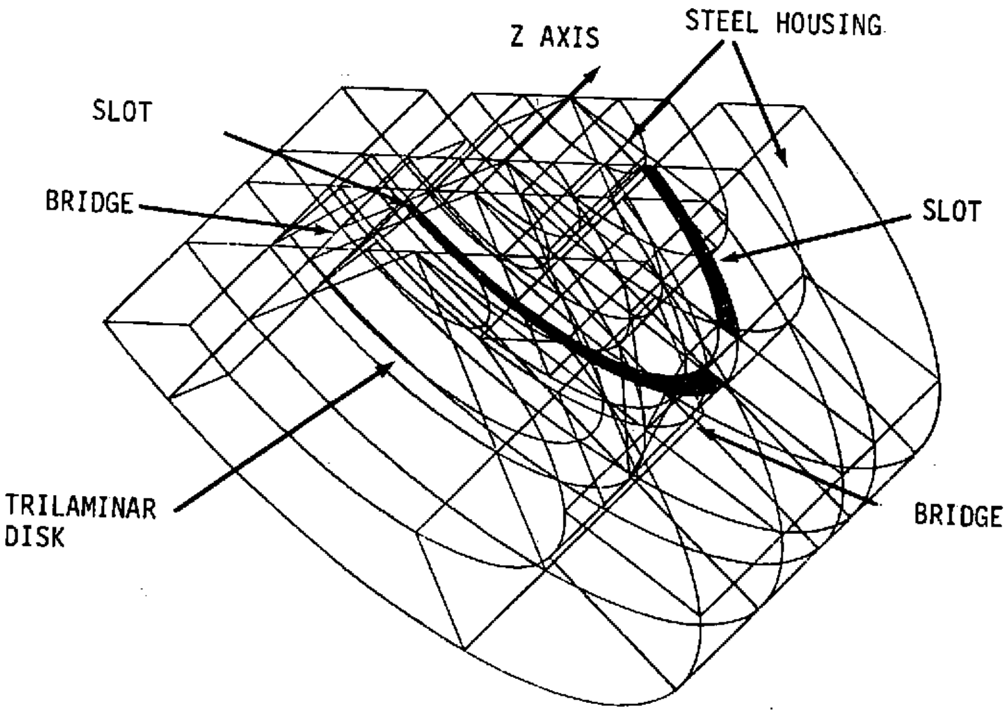

Fig. 4 - Finite element mesh of the hydrophone.

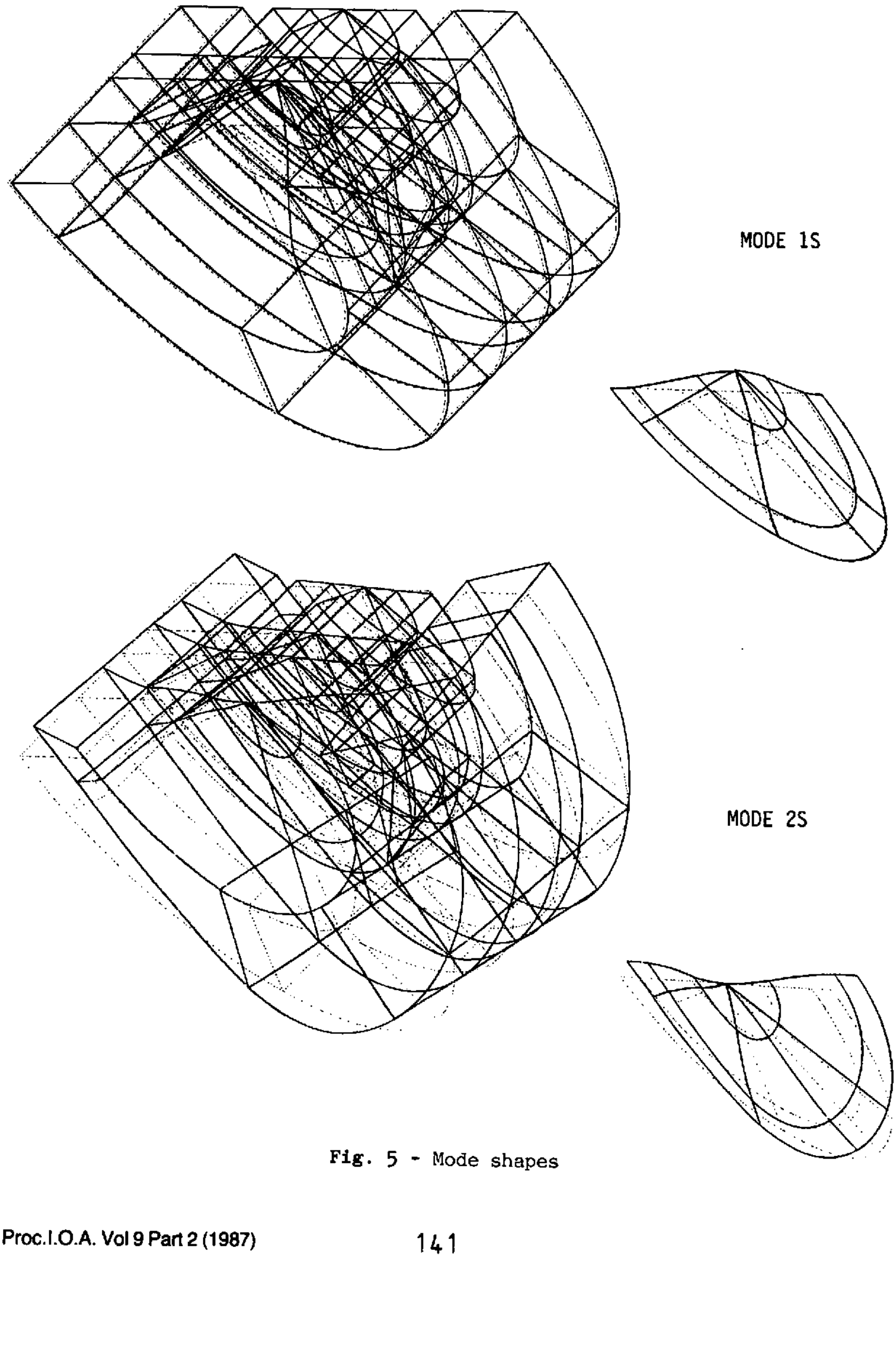

Fig. 5 - Mode shapes

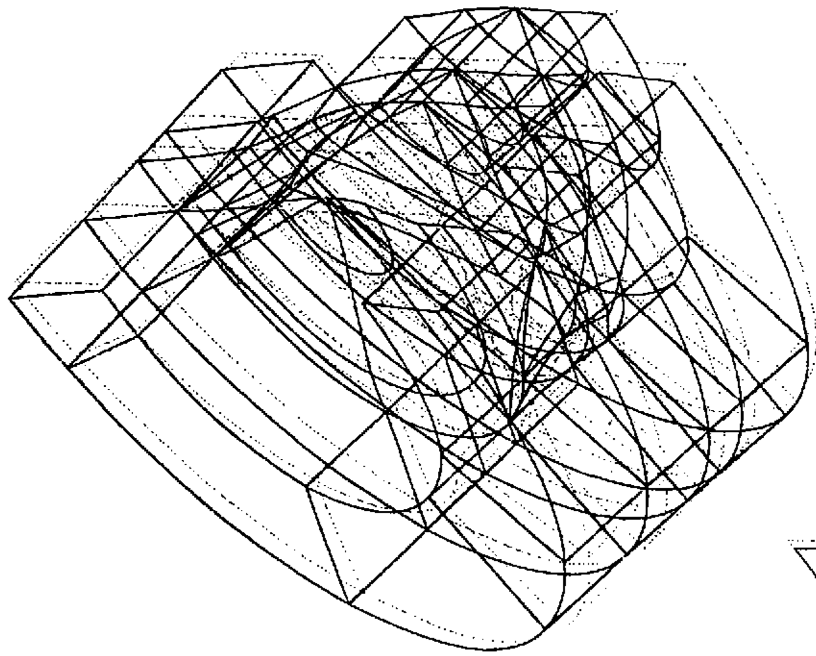

MODE 3S

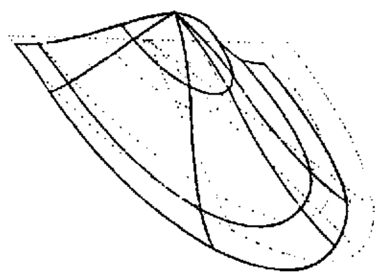

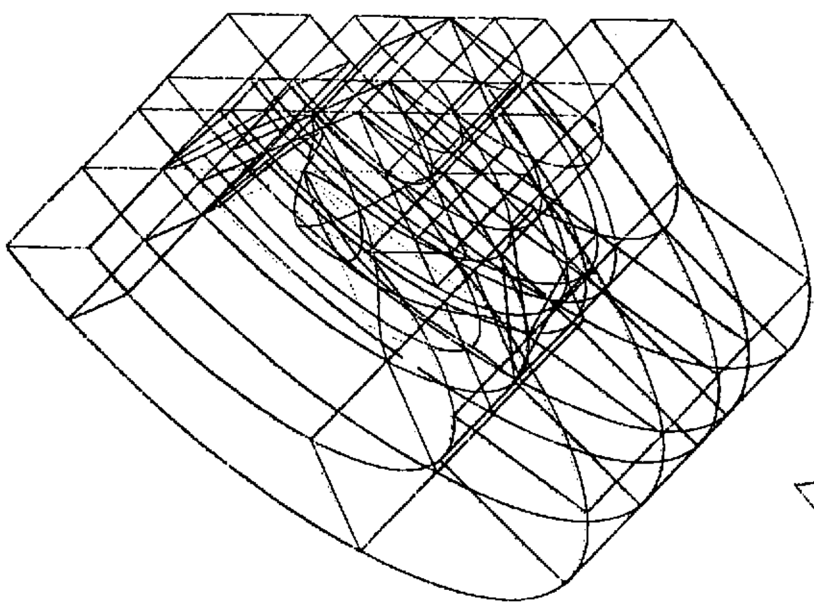

MODE 5S

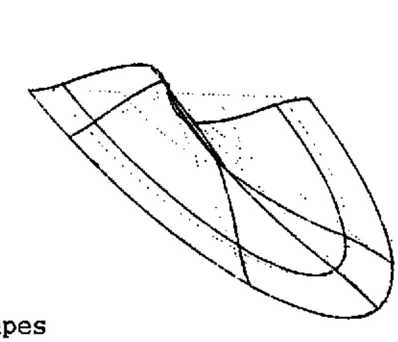

Fig. 5 (continued) - Mode shapes

obtained experimentally through an electrical excitation of the trilaminar disk, so that the strongly electrically coupled modes 1S and 3S have been clearly identified ; mode 2S, though weakly coupled, has been also significantly excited. The discrepancies between the computed and measured values of the eigenfrequencies of modes 2S and 3S can be partly imputed to the simplified description of the device taken into account in this finite element modelling.

The first in-air eigenfrequency (mode 2S)of the steel housing is 1.3 f_2 , i.e. is situated near the upper resonance frequency of the cardioïd hydrophone immersed in fluid and subjected to an incident wave (see preceding section):we may therefore infer that, in the upper part of the studied frequency range, the hypothesis of a perfectly rigid cylindrical housing is questionable.

CONCLUSION

If the lumped constant circuit and integral formulation modelling yields good results for the simplified hydrophone, it is not the same for the complete cardioïd hydrophone. The finite element modelling of the solid structure of the latter shows that the steel housing is not rigid in the upper part of the studied frequency range : this entails that a finite element modelling of the complete hydrophone (including the oil cavity and piezoelectricity) is necessary, the diffraction effects being taken into account through the integral equation formulation.

REFERENCES

(+) U.A. 253 au C.N.R.S.

[1] A. Defebvre, J. Pouliquen, final report, DRET Contracts 76/429 and 78/002, (1979)

[2] C. Granger, "Etude et réalisation d'hydrophones miniatures directifs". CNAM Thesis, Lille (1983)

[3] B. Stupfel, C. Granger, J.N. Decarpigny, final report, T.S.M. n° 83/1085, GERDSM, (1984)

[4] B. Stupfel, J.N. Decarpigny, first report, DRET Contract n° C.84.34.050.00.470.75.001 (1985)

[5] J.N. Decarpigny, J.C. Debus, B. Tocquet, D. Boucher, JASA, 78, 1499 (1985)

[6] B. Hamonic, R. Bossut, J.C. Debus, J.N. Decarpigny, D. Morel, P. Tierce, B. Tocquet, D. Boucher, 11th Seminar on Modal Analysis, Leuwen (Belgium) (1986)

[7] H.A. Schenck, JASA, 44 (1), 41 (1968)

[8] C. Granger, J.N. Decarpigny, final report n° C.83.48.826.163, GERDSM, (1985)

[9] P.M. Morse, Vibration and Sound, 2nd edition, Mc Graw Hill (1948).